

1 GIS-models with fuzzy logic for Susceptibility Maps of debris flow using multiple types of parameters: A Case Study
2 in Pinggu District of Beijing, China

3 Yiwei Zhang¹, Jianping Chen^{1,*}, Qing Wang¹, Chun Tan^{2,3}, Yongchao Li^{4,5,6}, Xiaohui Sun⁷, Yang Li⁸

4
5 1 College of Construction Engineering, Jilin University, Changchun 130026, China

6 2 China Water Northeastern Investigation, Design and Research Co., Ltd, Changchun, Jilin 130026, China

7 3 North China Power Engineering Co., Ltd. of China Power Engineering Consulting Group, Changchun, Jilin 130000,
8 China

9 4 Key Laboratory of Shale Gas and Geoenvironment, Institute of Geology and Geophysics, Chinese Academy of
10 Sciences, China.

11 5 University of Chinese Academy of Sciences.

12 6 Innovation Academy for Earth Science, Chinese Academy of Sciences, China.

13 7 Department of Earth Sciences and Engineering, Taiyuan University of Technology, Taiyuan 030024, China

14 8 Beijing institute of geological and prospecting engineering, Beijing 100020, China

15 * Corresponding author. Tel.:+86 13843047952

16 * Email address: chenjp@jlu.edu.cn

17
18
19 **Abstract**

20 Debris flow is one of the main causes of life loss and infrastructure damage in mountainous areas, this hazard
21 must be recognized in the early stage of land development planning. According to field investigation and expert
22 experience, a scientific and effective quantitative susceptibility assessment model was established in Pinggu District
23 of Beijing. This model is based on Geographic Information System (GIS), combining with grey relational, data-
24 driven and fuzzy logic methods. The inherent influence factors, which are divided into two categories, are selected
25 in the model consistent with the system characteristics of debris flow gully and one new important factor are proposed.
26 The results of the 17 models are verified by results published by the authority, and validated by two other indexes as
27 well as Area Under Curve (AUC). Through the comparison and analysis of the results, a method to optimize is
28 proposed, including reasonable application of field investigation and expert experience, simplification of factors and
29 scientific classification. And the final optimal susceptibility map with full discussion has the potential help in
30 determining regional-scale land use planning and debris flow hazard mitigation for decision makers, with full use of
31 insufficient data, scientific calculation, and reliable results. The model has advantages in economically backward
32 areas with insufficient data in mountainous areas because of its simplicity, interpretability and engineering usefulness.

33 Key words: debris flow; susceptibility assessment; fuzzy logic; model optimization; hazard mitigation

35 1 Introduction

36 Debris flows are processes of rapid transport of water and soil materials in mountain watersheds, with sudden
37 and destructive outbreaks(Di et al., 2019). Some debris flows can often cause devastating disasters and huge
38 losses(Zhang et al., 2021) and seriously threaten the lives and properties of the people in the mountains, the safety of
39 major projects, and restrict social and economic development (Iverson, 1997; Hungr et al., 2005; Hu et al., 2011;
40 Takahashi, 2014; Wu et al., 2019). Mass movements in Beijing range in scale from shallow slope failures and rockfalls
41 to catastrophic rock avalanches frequently mobilize to form debris flows, threatening the ecological environment of
42 the mountainous area (Zhong et al., 2004). Especially, in recent years, due to the superposition of extreme rainstorm
43 weather and human engineering activities, debris flow events have increased gradually(Li et al., 2021b). As the capital
44 of China, Beijing also has strong influence and radiation at home and abroad, where geological disasters are widely
45 concerned (Xie et al., 2004; Li et al., 2020b). With the deepening understanding of debris flow disaster and the
46 updating of database, a new and more accurate evaluation is also very necessary. Therefore, it is of great significance
47 to establish accurate and scientific debris flow susceptibility map.

48 Through previous studies, it can be summarized that the current research on debris flow mainly focuses on the
49 following aspects: study on mechanism of debris flow, study on early warning and prediction of debris flow, study
50 on numerical simulation of debris flow and study on debris flow hazard analysis. Especially, studies on debris flow
51 hazard analysis have raised the attention of the researchers as soon as it appears(Dong et al., 2009). Communicating
52 information about debris flow hazard analysis is a crucial component of preparedness and hazard mitigation (Chiou
53 et al., 2015). Susceptibility assessment, an important part of a hazard assessment of geological processes is more
54 flexible(Li et al., 2021a). In the early days, the susceptibility assessment of debris flows was mainly qualitative
55 research using geomorphological information (Guzzetti et al., 1999). In 1976, the United Nations commissioned the
56 International Union of Engineering Geology to conduct a risk assessment of debris flows, which marked the
57 beginning of research on the susceptibility assessment of debris flows as an important research direction for disaster
58 prevention and prediction (Li et al., 2020b). Many methods and techniques have been proposed to evaluate debris
59 flow susceptibility assessment based on different qualitative and quantitative approaches and geo-environmental
60 information (Liu and Wang, 1995), Such as the analytic hierarchy process (Wu et al., 2016), logistic regression
61 method (Regmi et al., 2013; Conoscenti et al., 2015), information value (Akbar and Ha, 2011; Melo et al., 2012),
62 support vector machine(Pourghasemi et al., 2017), frequency ratio (FR) (Sun et al., 2018), certainty factor (CF)
63 (Tsangaratos and Ilia, 2015), neural network (Lee et al., 2003; Liu et al., 2005) and Bayesian network algorithm
64 (Liang et al., 2012; Tien Bui et al., 2012), etc. These methods have corresponding advantages and limitations for
65 research subjects with different geological conditions. Generally speaking, it is easier to get satisfactory results by
66 combining and comparing various methods (Meyer et al., 2014; Di Napoli et al., 2020; Fang et al., 2020). In summary,
67 with the development of mathematical theory, the susceptibility assessment of debris flows has been extensively and
68 quantitatively studied, and the research methods have also changed from single to comprehensive.

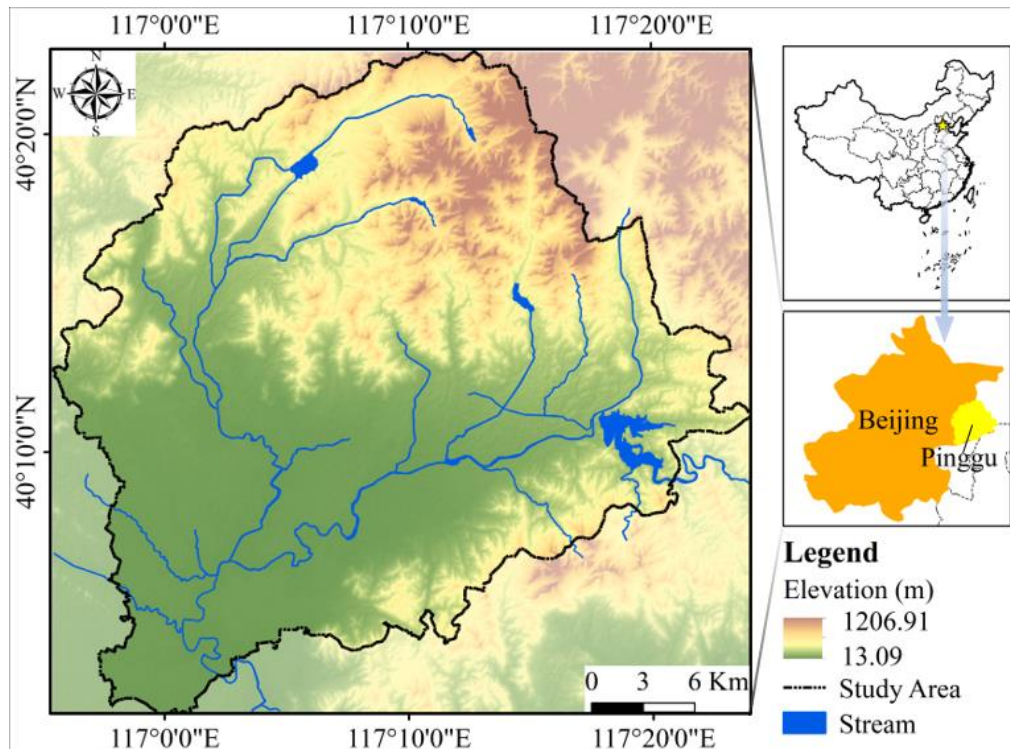
69 The economy in mountainous areas is often backward, we cannot supervise and verify every basin due to the
70 limited funds. The debris flow susceptibility assessment can give decision makers a basis for rational allocation of
71 resources, and determine which gullies should be focused on. In other words, the study plays a link role for other

72 studies. Recently, with the development of mathematical theory, computer technology, the application of 3S (Remote
73 sensing, Geography information systems, Global positioning systems), the susceptibility assessment of debris flows
74 has been extensively and quantitatively studied(Li et al., 2020a). As research progresses, debris flows are increasingly
75 seen as an open system. There are many factors influencing the system and the combination of factors is non-linear
76 and the interactions are chaotic. Therefore, it is very difficult to find a unified and standard evaluation model. At
77 present, when the information is insufficient, the field investigation and experience of experts are necessary. However,
78 the experience is often subjective and needs a lot of professional experience accumulation. It is very important to
79 express the experience of experts objectively and understandably to serve decision makers. The application of fuzzy
80 set theory in GIS environments is effective for similar problems(Luo and Dimitrakopoulos, 2003; Porwal et al., 2006).

81 The main objective of this paper is to propose a quantitative geographic information system (GIS)-based model.
82 The results of expert experience scoring and site surveys are used as guidance and reference in the modelling process.
83 We have tried to apply methods that can indicate the non-linearity of the debris flow system. Finally, the modelling
84 process should respect the laws of geomorphological evolution and the geological basis. Otherwise, the result will
85 tend to be simply data fitting(Porwal et al., 2006).

86 **2 Study area**

87 The study area is located on the northeast of Beijing, China (Fig. 1), with a total area of 948.24 square kilometers.
88 The elevation of Pinggu is high in the northeast and low in the southwest. It is surrounded by mountains, accounts
89 for about two-thirds of the total area, on three sides in the southeast and north. The central and southern parts are
90 alluvial plains. The area, geologically, is the west extension of the famous Jixian section, whose bedrock is mainly
91 Middle and Late Proterozoic dolomite(Lü et al., 2017). The administrative unit of Pinggu District is used as the study
92 area boundary, mainly considering that geological hazards frequently influence human economic activities, so
93 political factors must be taken into account. And within the administrative region, inconsistent decision-making can
94 be effectively avoided.

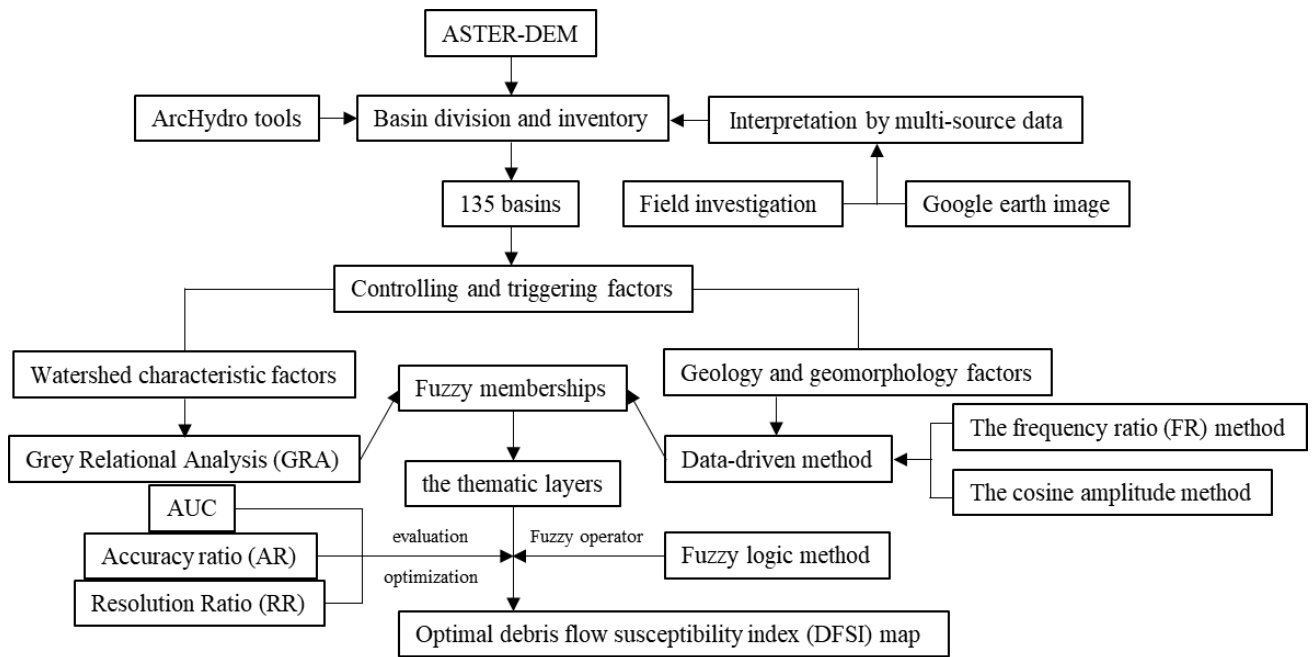


95
96 Fig. 1 Study area

97 **3. Data and Methodology**

98 In this study, the susceptibility assessment of debris flow hazard was based on the drainage basin unit. In a debris
 99 flow susceptibility assessment model, hydro-logical response unit can fully represent the hydrological process of
 100 hillside and will make the results more meaningful(Khan et al., 2013; Khan et al., 2016; Zou et al., 2019). First,
 101 drainage networks were extracted from the ASTER-DEM by using the ArcGIS ArcHydro Toolbox and regions
 102 without obvious watershed characteristics were directly deleted. Then for each drainage basin, 19 controlling and
 103 triggering factors divided into two types were calculated. In addition, for these factors have different characteristics,
 104 different methods were used to calculate the fuzzy membership for different type factors. Field investigation is
 105 generally required in geological hazard surveys. If the data from the field investigation is applied to the model, it can
 106 help the model building and reduce the time for model training. The weights derived from the grey relational analysis
 107 method used in the following section (section 3.4.1) are based on the data from the field investigation. While geology
 108 and geomorphology factors are independent of watershed characteristics, it is suitable to use statistical methods to
 109 determine the objective weight. Finally, the debris flow susceptibility index (DFSI) map was derived by overlaying
 110 the factor thematic layers with fuzzy logic method. The workflow of debris flow susceptibility assessment is showed
 111 in Fig.2. First, a DEM map of the Pinggu area was downloaded. Then, the basin units were generated from the DEM
 112 map using the ArcHydro tool. The derived results were analyzed and units that did not fit the characteristics of the
 113 watershed were removed. During the analysis, the field investigation data and Google images were referenced. After
 114 that, the controlling and triggering factors for the remaining 135 catchments were counted. For the fuzzy
 115 memberships, watershed characteristic parameters were determined by grey correlation and the geological and
 116 geomorphological factors were determined by the frequency ratio (FR) method and the cosine amplitude method.
 117 Finally, the individual layers were overlaid by fuzzy logic operations to obtain the final map. As there were different

118 combinations of factors, 17 results were derived. Three indexes (AUC, AR and RR) were used to evaluate advantages
 119 and disadvantages of these results.



120
 121 Fig.2 Workflow of debris flow susceptibility assessment

122 **3.1 Debris flow basin division and inventory**

123 There are many geological hazard points in mountainous area, so it is not realistic to monitor them completely
 124 by professional teams. According to the monitoring and preventing staff and the villagers, the detailed field
 125 investigation (Fig.3) for the evidence collection of debris flows will be carried out at the reported disaster point,
 126 aiming at record the loose material, delineating the basin and exploring other important information of the debris
 127 flow gullies. Moreover, field investigation is also very important for model modification. Then based on the
 128 Hydrology module in ArcGIS 10.2, the research object can be determined. Compared with grid unit and slope unit,
 129 hydrological response unit for susceptibility of debris flow has greater advantages(Li et al., 2021b; Zou et al., 2019).
 130 Finally, 135 basins are divided after removing the flat and irregular areas (Fig. 4), referring to the result of the field
 131 investigation and the remote sensing image. In the 135 basins, 48 basins were investigated on field, accounting for
 132 36%.

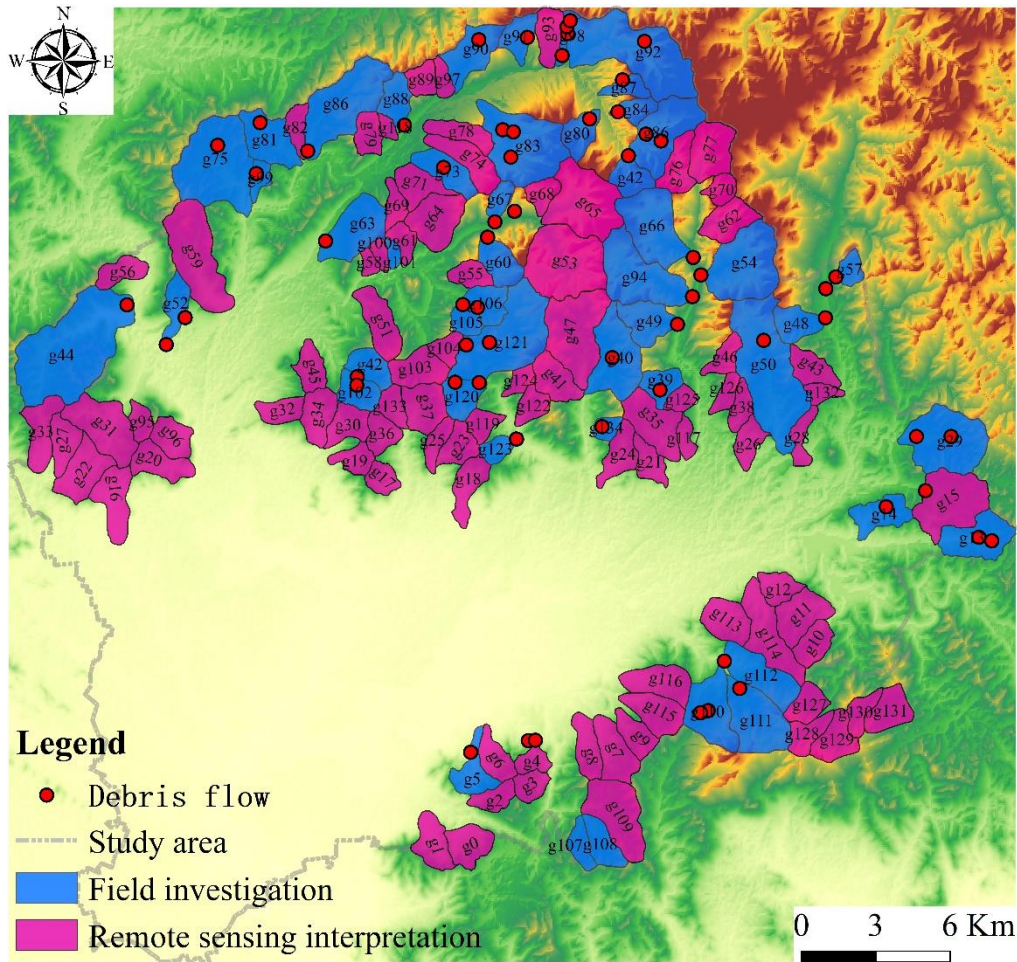


133

134 Fig.3 Field investigation photos. **a** Loose material; **b** Middle and Late Proterozoic dolomite; **c** colluvium deposit; **d**

135 Slope fracture; **e** Channel erosion phenomenon

136



137

138 Fig. 4 Debris flow basin division and inventory.

139 Note: The data of debris flow points comes from Beijing Municipal Commission of Planning and Natural Resources
 140 websites (http://ghzrzyw.beijing.gov.cn/zhengwuxinxi/zxzt/dzzhfztt/zzzhdcpg/202008/t20200807_1976436.html)

141 **3.2 Debris flow controlling and triggering factors**

142 The basic requirement for the assessment of debris flows is that some factors included are easily obtainable, are
 143 meaningful for susceptibility assessment, and can be used for evaluating the need for passive or active debris flow
 144 mitigation. According to previous studies, 19 factors are selected in this study. the factors are divided into two types
 145 (Table 1) because of their different characteristics. Watershed characteristic factors (Type A) can be directly
 146 quantified, once the basin is determined (Fig. 5). The influence of these parameters is bounded by the watershed;
 147 Geology and geomorphology factors (Type B) need to be further processed, even if the watershed is determined. The
 148 scope of these parameters is independent of the watershed boundary.

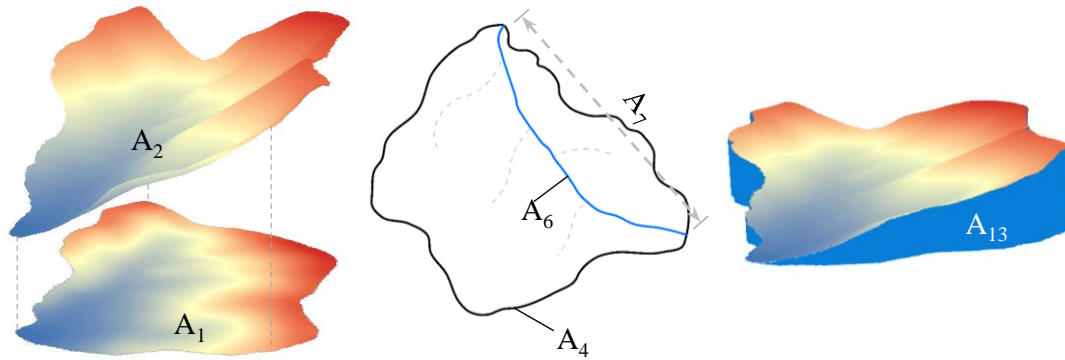
149

150 Table 1 Factors for susceptibility assessment

Factors and Description		Significance	obtaining ways
A ₁	The planimetric (projected) area of the catchment	Geometric parameter; affecting the accumulative total volume of water and representing the potential magnitude(Zhang et al., 2011; Cao et al., 2016; Chang and Chien, 2007)	derived from DEM
A ₂	The curved surface area of the catchment	Real contact area between rainfall and basin	derived from DEM
A ₃	The surface roughness of the catchment	Dimensionless parameters, reflecting the fragmentation degrees of the surface and the ground surface micro-topography. Wu et al. (2019) believe the factor can further reflects the ability of the earth to resist wind erosion.	Calculated by $A_3 = A_2 / A_1$
A ₄	The perimeter of catchment	Geometric parameter, controlling the boundaries of a watershed	derived from DEM
A ₅	Form factor	Hydrologic parameter, related to the distribution of flow rate hydrograph(Chang and Chien, 2007)	Calculated by $A_5 = \frac{A_4}{2\sqrt{\pi A_1}}$
A ₆	The curve length of the main channel	Importance for the travel distance of materials and affecting the potential of erosive agents to dislodge and transport materials(Gómez and Kavzoglu, 2005)	derived from DEM
A ₇	The straight length of the main channel	Geometric parameter, representing the change of material source in space	derived from DEM
A ₈	Bending coefficient of the main channel	Affecting the discharge situation of debris flows(Li et al., 2020a; Zhang et al., 2013)	Calculated by $A_8 = A_6 / A_7$
A ₉	The gradient of the main channel	Hydraulic gradient parameter, affecting water transport capacity	Calculated by $A_9 = A_{12} / A_6$
A ₁₀	Maximum elevation in the catchment	Affecting vegetation and bedrock exposure	derived from DEM
A ₁₁	Minimum elevation in the catchment	Affecting vegetation and bedrock exposure slightly	derived from DEM
A ₁₂	Maximum relative relief in the catchment	The higher the value of A ₁₂ is, the large relative relief provides favorable terrain conditions for the initiation of the debris flow source.	Calculated by $A_{12} = A_{10} - A_{11}$
A ₁₃	Basin volume: the volume above the level of the minimum elevation in the basin	Representing the maximum material source that can be produced in an ideal state, loose material volume	derived from DEM
A ₁₄	Drainage density	Representing the geological structure, lithology, and the degree of rock weathering comprehensively and affecting the	the ratio of the total length of river network lines to A ₁

range of lateral erosions and retrogressive(Cao et al., 2016; Zhang et al., 2011)				
Geology and geomorphology factors (Type B)	B ₁	Lithology	Affecting the rock mass shear strength and permeability (Donati and Turrini, 2002)	derived from 1:50,000 geological maps
	B ₂	Proximity to faults	correlated with slope failures by generally reducing the strength of the rock mass (Dramis and Sorriso-Valvo, 1994; Korup, 2004; Kellogg, 2001; Kritikos and Davies, 2015).	derived from 1:50,000 numerical geological maps
	B ₃	Slope (degrees)	correlated with the probability of landslide occurrence (Dai and Lee, 2002; Lee and Choi, 2004; He and Beighley, 2008). The greater the slope, the greater the vertical component of gravity (Donati and Turrini, 2002), and the higher frequency of slope failures (Lee and Sambath, 2006; Lee and Talib, 2005)	derived from DEM
	B ₄	Slope aspect	affecting slope instability directly or indirectly, as a result of drying winds, sunlight, rainfall and vegetation (Dai and Lee, 2002; Dai et al., 2001).	derived from DEM
	B ₅	Curvature	Affecting slope stability. While Lee and Talib (2005) and Ohlmacher (2007) argue on how curvature affect slope stability.	derived from DEM

151 Note: The geological maps are provided by Beijing institute of geological and prospecting engineering and the digital elevation model-(DEM) of study area are from
152 SRTM-DEM with a resolution of 30 m ([http://gdex. cr. usgs. gov/gdex/](http://gdex.cr.usgs.gov/gdex/)).
153



154
 155 Fig. 5 Graphical illustration of some Type A factors. A_1 is the planimetric (projected) area of the catchment; A_2 is
 156 the curved surface area of the catchment; A_4 is the perimeter of catchment; A_6 is the curve length of the main
 157 channel; A_7 is the straight length of the main channel; A_{13} is basin volume

158 3.3 Fuzzy logic in susceptibility modelling

159 Fuzzy set theory is proposed by Zadeh (1965). It is an efficient way of expressing the concept of partial set
 160 membership degree. This concept differs from classical binary (0-1 value) logic. More words with a transitional fuzzy
 161 descriptions (such as low, medium, and high) are used (Kritikos and Davies, 2015). This fuzzy expression is
 162 particularly applicable to geological hazard classification. In the theory of fuzzy sets, elements have different degrees
 163 of membership in the interval [0,1]. 1 represents complete membership, and 0 represents non membership. Ross
 164 (1995) showed that fuzzy systems are useful in two general situations (Kritikos and Davies, 2015). The method is
 165 very consistent with the characteristics of debris flow system, whose predisposing factors are fuzzy in nature and
 166 mechanism is complex and not fully understood. Application of fuzzy logic method, the critical step is to find the
 167 suitable fuzzy membership of factors. And fuzzy membership degree is equivalent to the weight in expert scoring
 168 method, which is calculated by objective method rather than given subjectively.

169 3.4 Fuzzy memberships

170 3.4.1 Grey Relational Analysis (GRA) in susceptibility modeling

171 GRA is proposed by Deng (1982) and it is an important part of grey system theory (Wang et al., 2014).
 172 Comparing with mathematical statistics methods which need lots of sample data, typical probability distribution and
 173 large calculation, GRA is applicable to small sample size and whether the data is regular or not. There will be no
 174 inconsistency between qualitative analysis and quantitative analysis (Deng, 1988). Besides it is to excoitate the
 175 leading and potential factors that affect the development of the system, and quantitatively describe the development
 176 and change trend of the system by studying whether the relative change trend of the grey factor variables with
 177 complex relationship is consistent in the process of system development and evolution (Liu et al., 2004). Thus, grey
 178 correlation analysis is introduced to quantify the correlation between each factor and the evaluation results according
 179 to field investigation expert experience. First, the procedure of GRA is to translate the performance of every
 180 alternative into a comparability sequence (Lin and Lin, 2002; Kuo et al., 2008; Wei et al., 2017). Therefore, according
 181 to technical standard, "Specification of geological investigation for debris flow stabilization (DZ/T0220-2006)",
 182 published by the China Ministry of Lands and Resources, the preliminary assessment results of debris flow

183 susceptibility are obtained, which are used as the reference sequence of grey relation method (Table 2). Second, the
 184 grey correlation coefficient of all A factors is calculated by Eq. (1). Finally, the average grey relational coefficient
 185 (the correlation degree) is calculated by Eq. (2) as the fuzzy memberships (Table 3).

$$186 \quad \xi_i(k) = \frac{\min_k \min |x_0(k) - x_i(k)| + 0.5 \max_k \max |x_0(k) - x_i(k)|}{|x_0(k) - x_i(k)| + 0.5 \min_k \min |x_0(k) - x_i(k)|} \quad (1)$$

187 Where $\xi_i(k)$ is the grey relational coefficient, $i=1, 2, \dots, n$ are the number i type A factors, $k=1, 2, \dots, n$ are the
 188 number of basins, $x_0(k)$ is the reference sequence (ideal target sequence), $x_i(k)$ is the number i type A factor sequence

$$189 \quad r_i = \frac{1}{N} \sum_{k=1}^n \xi_i(k) \quad (2)$$

190 Where r_i is the correlation degree in the range (0,1). N is the total number of basins in Table 2

Table 2 Quantitative evaluation grade standard table for Debris flow susceptibility

name	g5	g13	g14	g29	g39	g40	g42	g44	g48	g49	g50	g52	g54
score	59	54	50	63	61	66	55	65	78	69	85	46	70
name	g57	g60	g63	g66	g67	g72	g73	g75	g80	g81	g83	g84	g85
score	56	63	58	73	62	84	62	67	84	69	80	75	86
name	g86	g87	g88	g90	g91	g92	g94	g98	g99	g101	g102	g105	g106
score	73	84	60	70	80	84	71	78	61	65	67	65	70
name	g107	g108	g110	g111	g112	g120	g121	g123	g134	-	-	-	-
score	45	45	69	69	74	62	63	73	56	-	-	-	-

191 Note: $(130 \geq \text{score} \geq 116, \text{VH})$, $(115 \geq \text{score} \geq 87, \text{M})$, $(86 \geq \text{score} \geq 44, \text{L})$, $(43 \geq \text{score} \geq 15, \text{N})$
 192 VH=very high susceptibility, M=moderate susceptibility, L=low susceptibility, N= Non-debris flow
 193

194 Table 3 The fuzzy memberships of type A factors

Factor	A ₁	A ₂	A ₃	A ₄	A ₅	A ₆	A ₇
Fuzzy membership	0.77	0.77	0.63	0.6	0.54	0.55	0.67
Factor	A ₈	A ₉	A ₁₀	A ₁₁	A ₁₂	A ₁₃	A ₁₄
Fuzzy membership	0.71	0.55	0.55	0.59	0.61	0.79	0.54

195

196 3.4.2 Data-driven method in susceptibility modeling

197 landslide is one of the main fixed sources of debris flow in mountainous area. Shallow landslides are one of the
 198 most common categories of landslides. They frequently involve large areas and different soils in various climatic
 199 zones (Benda and Dunne, 1987; Selby, 1982; Borrelli et al., 2014). Great debris flows may result from numerous,
 200 small slope failures that subsequently coalesce (Fairchild, 1987; Roeloffs, 1996), from flow enlargement due to
 201 incorporation of bed and bank debris (Pierson et al., 1990; Bovis and Dagg, 1992), or from large, individual landslides
 202 that mobilize partially or almost totally (Vallance and Scott, 1997; Iverson et al., 1997). Debris flows may also scour
 203 steep channels to bedrock and accelerate sediment delivery to downstream, lower-gradient channels. The spatial and
 204 temporal distribution of shallow landslides are important controls on landscape evolution and a major component of
 205 both natural and management-related disturbance regimes in mountain drainage basins (Tsukamoto et al., 1982;
 206 Dietrich et al., 1986; Benda, 1987; Crozier et al., 1990). Therefore, the landslide susceptibility assessment methods
 207 can be used for reference to debris flow susceptibility assessment.

208 For type B factors which cannot be characterized by a specific number, the frequency ratio (FR) method and the

209 cosine amplitude method can be used to derive their fuzzy memberships. The FR ratio defined as Eq. (3). Considering
 210 the fuzzy membership must be in the interval [0,1], the FR values of the different categories are normalized by the
 211 largest FR value (Lee, 2006; Pradhan, 2010, 2011a, b) within the same type factor (Table 4) in order to derive the
 212 function.

$$213 \quad FR = \frac{N_{(Di)}/N_{(Ci)}}{N_{(D)}/N_{(A)}} \quad (3)$$

214 where $N_{(Di)}$ is the number of debris flow pixels in the category i , $N_{(Ci)}$ is the total number of pixels in the category
 215 i , $N_{(D)}$ is total number of debris flow pixels in the study area, and $N_{(A)}$ is the total number of pixels in the study area.
 216

217 The cosine amplitude method (Ross, 1995) is also widely used (Ercanoglu and Gokceoglu, 2004; Kanungo et
 218 al., 2006; Kanungo et al., 2009; Ercanoglu and Temiz, 2011) to establish relationships among elements of two or
 219 more datasets (Kritikos and Davies, 2015). Assuming that n is the number of data samples (categories of a factor
 220 used in the analysis) represented as an array $X = \{x_1, x_2, \dots, x_n\}$ and that each of its elements, x_i , is a vector of length
 221 m (i.e. the size of the raster image) and can be expressed as $X = \{x_{i1}, x_{i2}, \dots, x_{im}\}$, then each element of a relation r_{ij}
 222 results from a pairwise comparison of a factor category x_i with a category of the debris flow distribution layer x_j
 223 (debris flow or non-debris flow). The memberships can be calculated by Eq. (4):

$$224 \quad r_{ij} = \frac{|\sum_{k=1}^m x_{ik}x_{jk}|}{\sqrt{(\sum_{k=1}^m x_{ik}^2)(\sum_{k=1}^m x_{jk}^2)}} \quad (4)$$

225 Analogy with the study of Kanungo et al. (2006), we defined the r_{ij} value for any given factor category as the
 226 ratio of the total number of debris flow pixels in the category to the square root of the product of the total number of
 227 pixels in that category and the total number of debris flow pixels in the area. Values of r_{ij} close to 1 indicate similarity
 228 whereas values close to 0 indicate dissimilarity between the two datasets (Kritikos and Davies, 2015). What's more,
 229 every thematic layer must use the same pixel size to use the method properly.
 230

Table 4 Factor categories and their fuzzy membership degrees

Factor	Factor class	Number of pixels	Number of pixels %	Number of pixels classified as debris flows	Number of pixels classified as debris flow %	Frequency ratio (FR)	Normalized frequency ratio	r_{ij}	Comprehensive ratio (FRR)
Lithology	Quaternary sediments-unconsolidated clastic sediments	7562017	0.320	48190	0.017	0.026	0.021	0.091	0.002
	Coarse-grained sediments	1148321	0.049	21741	0.008	0.076	0.063	0.061	0.004
	Medium-grained sediments	259619	0.011	12013	0.004	0.186	0.154	0.045	0.007
	Fine-grained sediments	754655	0.032	76380	0.027	0.407	0.337	0.114	0.038
	High-grade metamorphics	986435	0.042	154332	0.055	0.629	0.522	0.162	0.085
	Granitoids	725651	0.031	140936	0.050	0.781	0.648	0.155	0.100
	Mafic extrusive	75495	0.003	16398	0.006	0.873	0.724	0.053	0.038
	Terrigenous clastic rock	3289458	0.139	986495	0.352	1.205	1.000	0.41	0.410
proximity to faults	Limestones	8804379	0.373	1343754	0.480	0.614	0.509	0.478	0.243
	<100	1057209	0.045	231016	0.083	0.878	1.000	0.198	0.198
	100-500	3778095	0.160	774566	0.277	0.824	0.938	0.363	0.341
	500-1000	3894600	0.165	716963	0.256	0.740	0.842	0.349	0.294
	1000-2000	5707265	0.241	760699	0.272	0.536	0.610	0.36	0.220
	2000-3000	2749240	0.116	246925	0.088	0.361	0.411	0.205	0.084
slope (degrees)	>3000	6421103	0.272	69382	0.025	0.043	0.049	0.109	0.005
	0-5	9674508	0.410	153889	0.055	0.064	0.056	0.162	0.009
	5-10	2815606	0.119	383198	0.137	0.547	0.480	0.255	0.123
	10-15	2955913	0.125	521040	0.186	0.709	0.622	0.298	0.185
	15-20	2879704	0.122	570515	0.204	0.797	0.699	0.312	0.218
	20-25	2432724	0.103	498303	0.178	0.824	0.723	0.291	0.210
	25-30	1620325	0.069	350686	0.125	0.870	0.764	0.244	0.187
	30-35	837185	0.035	209574	0.075	1.007	0.883	0.189	0.167
	35-40	294141	0.012	82000	0.029	1.121	0.983	0.118	0.116
	40-45	77038	0.003	21133	0.008	1.103	0.968	0.06	0.058
Slope aspect	>45	30091	0.001	8529	0.003	1.140	1.000	0.038	0.038
	Flat	380875	0.016	463	0.000	0.005	0.005	0.009	0.000
	North	2370048	0.100	296900	0.106	1.006	1.000	0.318	0.111
	Northeast	2193998	0.093	279917	0.100	0.513	0.510	0.218	0.092
	East	2873308	0.122	295555	0.106	0.414	0.411	0.224	0.111
	Southeast	3122267	0.132	353489	0.126	0.455	0.453	0.245	0.108

	South	3219111	0.136	354420	0.127	0.443	0.440	0.246	0.133
	Southwest	3144353	0.133	400064	0.143	0.512	0.509	0.261	0.135
	West	3525895	0.149	436381	0.156	0.498	0.495	0.273	0.140
	Northwest	2787380	0.118	381679	0.136	0.551	0.547	0.255	0.318
Curvature	Concave	490900	0.021	109157	0.039	0.893	1.000	0.136	0.136
	Less concave	2037602	0.269	394583	0.141	0.778	0.871	0.259	0.226
	Flat	18364429	15.992	1769210	0.631	0.387	0.433	0.549	0.238
	Less convex	2202019	8.482	416142	0.149	0.759	0.850	0.266	0.226
	Convex	522285	0.692	112740	0.040	0.867	0.971	0.139	0.135

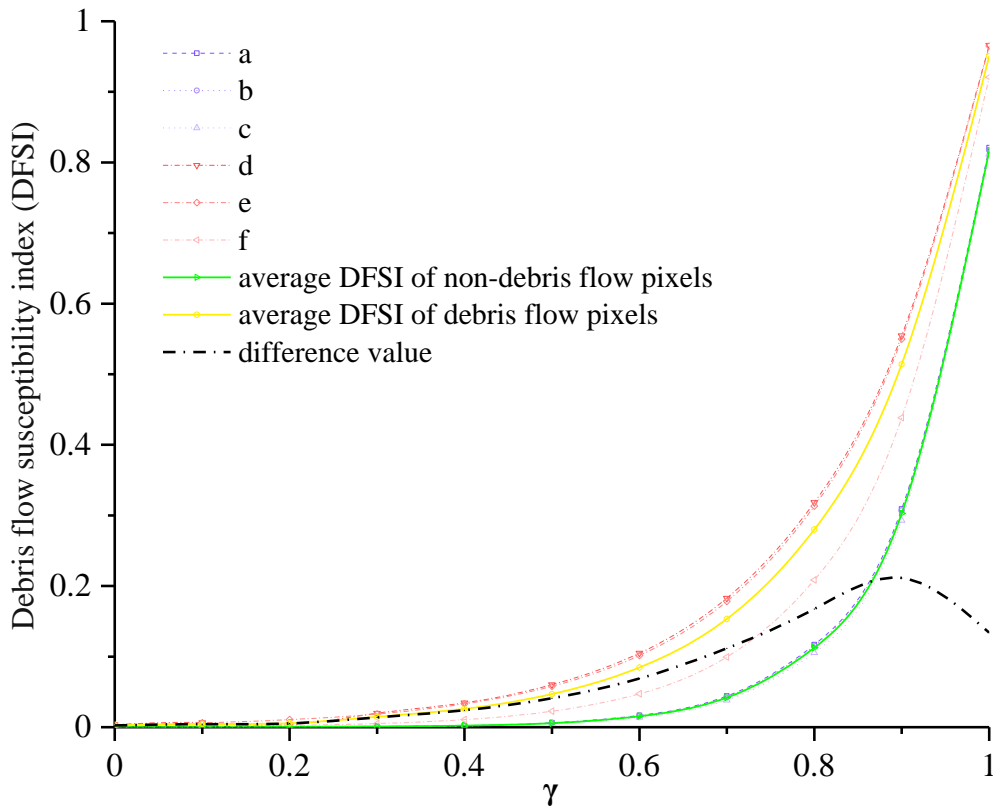
232

233 **3.5 DFSI map**

234 To derive the debris flow susceptibility index (DFSI) map by overlaying the factor thematic layers using fuzzy
 235 logic method, the "fuzzified" factors represented by information layers in raster format with values ranging from 0
 236 to 1 need to be combined. Compared with other four fuzzy operators, Fuzzy Gamma (Eq.5) is more suitable for the
 237 research (Kritikos and Davies, 2015). To determine the appropriate γ value, the results of different gamma values
 238 were compared by the greatest distance (Kritikos and Davies, 2015) between the average DFSI curves of the debris
 239 flows locations and non-debris flows locations (For example, flat pixels)(Fig. 6). Finally, 0.9 is determined for the γ
 240 value, because there is the greatest difference between debris flow and non-debris flows locations areas. In order to
 241 illustrate the superiority of our model through comparison, seventeen results are calculated in ArcGIS.

242
$$\mu_{(x)} = (1 - \prod_{i=1}^n (1 - \mu_i))^\gamma * (\prod_{i=1}^n \mu_i)^{1-\gamma} \quad (5)$$

243 where $\mu_{(x)}$ is the combined membership value, μ_i is the fuzzy membership function for the i th map, $i=1,2, \dots, n$
 244 are the numbers of thematic layers to be combined, and γ is a parameter in the range (0,1).



245 Fig. 6 Effect of γ value on Debris flow susceptibility index (DFSI). Curves d, e and f correspond to debris flow pixels,
 246 and curves a, b and c correspond to non-debris flow area where a Debris flow is unlikely. According to curve i, the
 247 maximum difference between the average DFSI values is observed for $\gamma \approx 0.9$
 248
 249

250 To find the optimal model, seventeen results were compared (Table 5). According to the distribution map of
 251 potential geological hazard points and susceptibility map in Pinggu District published by Beijing Municipal
 252 Commission of Planning and Natural Resources(Bmcp&Nr, 2020), three indexes are used to verify the validity and
 253 accuracy of the model.

254 The results of the model are independent of the model itself, so the predictive performance of the final map is

255 not just “the goodness of fit” of the data (Chung et al., 1995; Remondo et al., 2003). A relatively reliable technique
 256 for quantitatively assessing how well a model is the construction of validation or success rate curves (Chung and
 257 Fabbri, 1999; Westen et al., 2003; Remondo et al., 2003; Frattini et al., 2010) based on a comparison between the
 258 spatial distribution of debris flows and modelled debris flow susceptibility. The curves illustrate the debris flow
 259 recorded in the area with respect to susceptibility values also expressed as cumulative percentages of the total area.
 260 The area under the curve (AUC) defines the success rate (Marjanović et al., 2011). Generally, AUC values above 0.7
 261 indicate model performance can be acceptable, while below 0.7, the performance is considered poor (Kritikos and
 262 Davies, 2015).

263 Although AUC is an effective evaluation method, the results are not comprehensive as mathematical features
 264 for selecting the best measurement model because of insufficiency data for validation. In order to ensure the
 265 objectivity of the results, we can only effectively use the recorded debris flow gully as positive, while the others as
 266 negative. Thus, a two-category test is proposed to verify the model in this paper. First, the DFSI map of each model
 267 are divided into two categories by Natural Breaks (Jenks) method (Fig. 7). Then the accuracy ratio (AR) is defined
 268 as the frequency of the number of debris flow both classified by model and simultaneously recorded in site to the
 269 number of debris flow recorded in site. The Resolution Ratio (RR) is defined as the number of debris flow
 270 classified by model and simultaneously recorded in site to the total number debris flow classified by the model (in
 271 red color). Take R₄ for example, there are total 135 basins in the research area, but only 46 records of debris flows
 272 (Fig.3). And in the results of two categories by Natural Breaks (Jenks) method, 20 basins are divided in to debris
 273 flow, while there are only 14 debris flows among them. Then AR is calculated by dividing 14 into 46 and RR was
 274 calculated by dividing 14 into 20.

275 The higher the two values, the better the susceptibility map. Finally, the performance of models (P value) can
 276 be obtained by the Eq. (6). AUC values less than 0.6 are directly eliminated. Comparing the results of rest models,
 277 the result of R₁₆ is optimal, and the results of DFSI map are in good agreement with those of field investigation
 278 (Fig. 8).

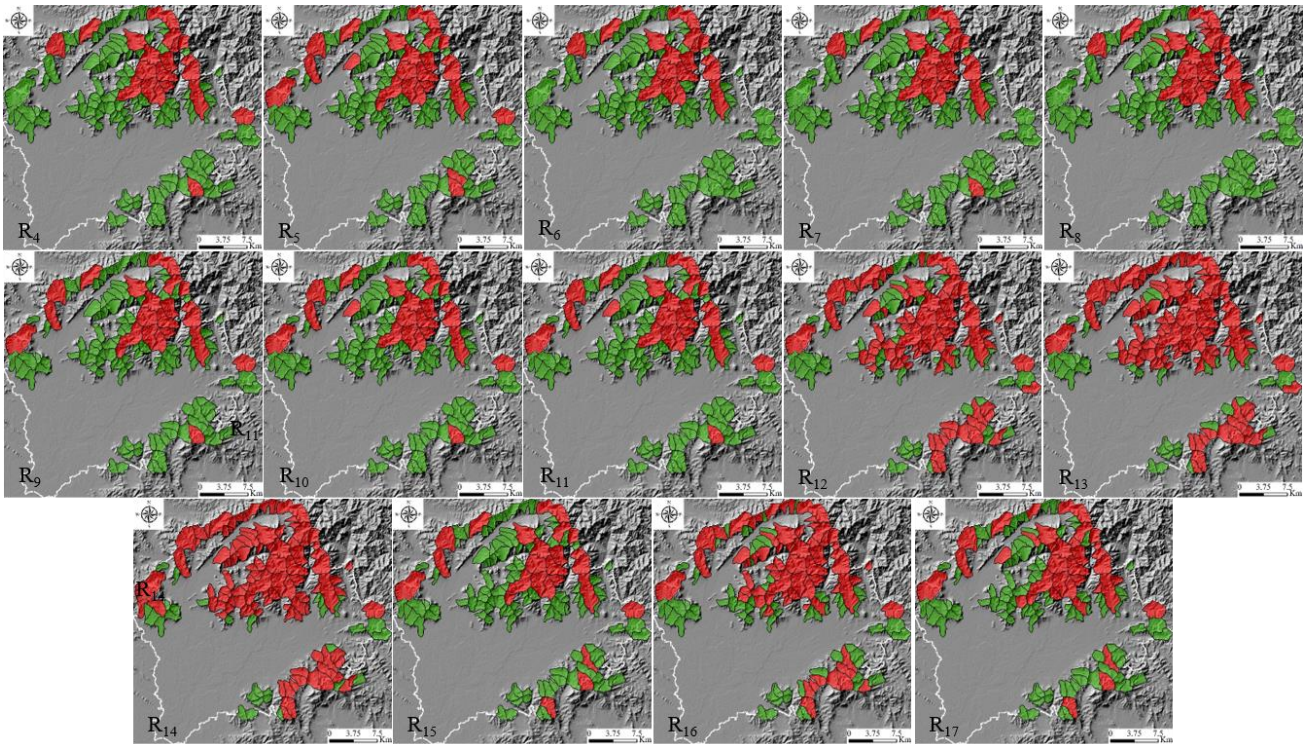
$$279 \quad P = AUC + \sqrt{(AR * RR)} \quad (6)$$

280 Table 5 Predictive performance of different models

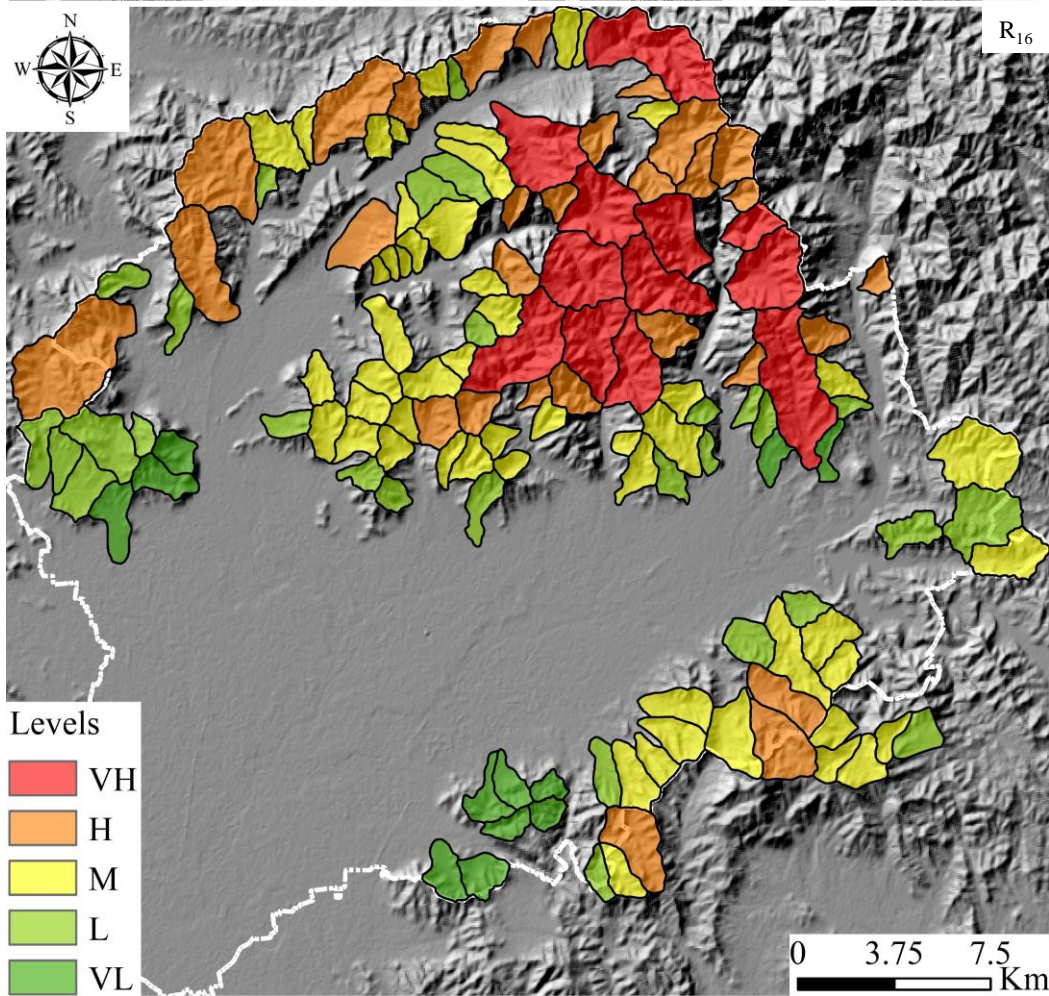
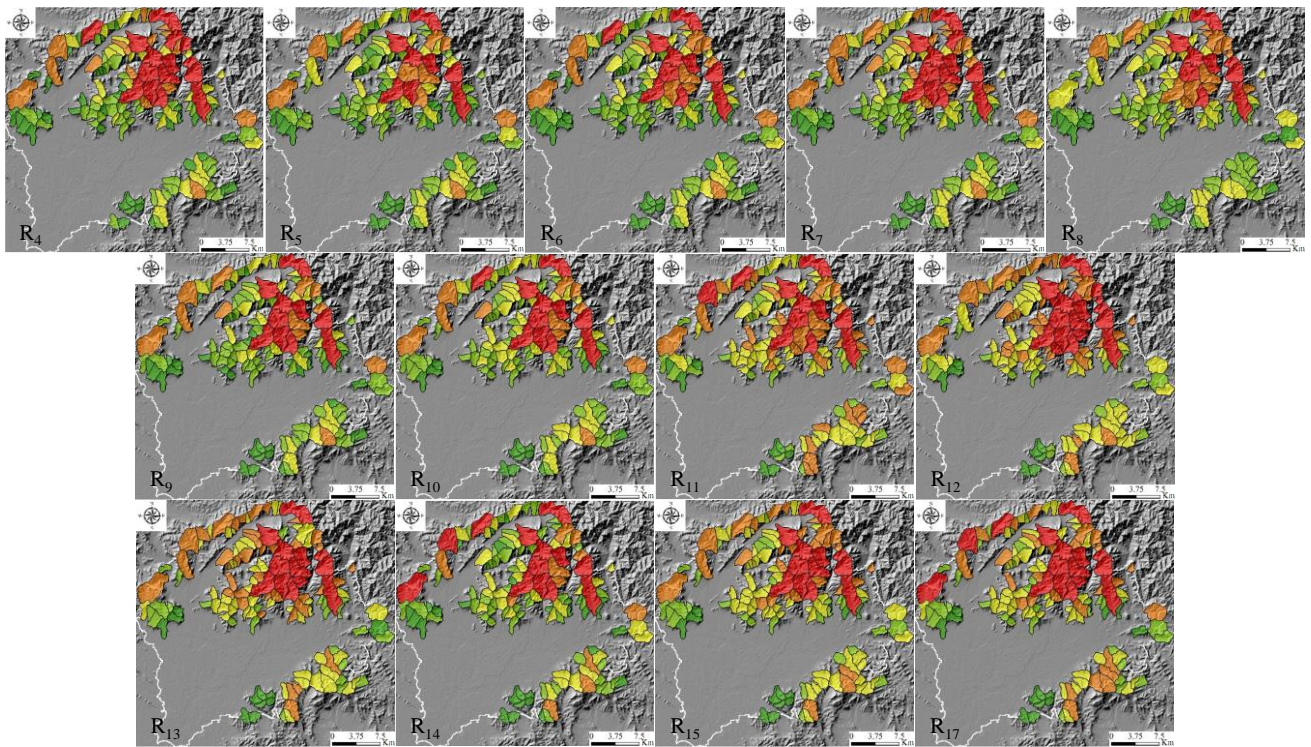
Result and Description			AUC	Two-category test		Performance index (centesimal grade)
				Accuracy Ratio (AR)	Resolution Ratio (RR)	
A factors only or B factors only	R ₁	B factors with r _{ij}	0.460	/	/	/
	R ₂	B factors with FR	0.687	/	/	/
	R ₃	B factors with FRR	0.602	/	/	/
	R ₄	All A factors	0.786	0.304	0.700	83
	R ₅	Selected A factors	0.760	0.391	0.750	94
All factors as a single thematic layer	R ₆	All A factors and B factors with r _{ij}	0.776	0.261	0.667	74
	R ₇	All A factors and B factors with FR	0.779	0.283	0.684	78
	R ₈	All A factors and B factors with FRR	0.753	0.326	0.600	76
	R ₉	Selected A factors and B	0.746	0.348	0.727	86

		factors with r_{ij}				
	R ₁₀	Selected A factors B factors with FR	0.761	0.348	0.727	87
	R ₁₁	Selected A factors B factors with FRR	0.740	0.348	0.727	85
A factors combined into one thematic layers, B factor combined into another thematic layers	R ₁₂	All A factors and B factors with r_{ij}	0.708	0.5	0.511	82
	R ₁₃	All A factors and B factors with FR	0.753	0.848	0.394	99
	R ₁₄	All A factors and B factors with FRR	0.711	0.870	0.404	96
	R ₁₅	Selected A factors and B factors with r_{ij}	0.726	0.348	0.667	80
	R ₁₆	Selected A factors and B factors with FR	0.768	0.739	0.442	100
	R ₁₇	Selected A factors B factors with FRR	0.740	0.457	0.600	88

281 Note: Selected A factors with fuzzy membership more than 0.6; FRR represents the product of FR and r_{ij} ; Performance
 282 index is normalized by the largest FR value
 283



284
 285 Fig.7 Results of two categories by Natural Breaks (Jenks) method



286

287
288

Fig. 8 Debris flow susceptibility maps. Note: AUC results of R₁-R₄ below 0.7 were not shown.

289

4 Results and Discussion

290 Through the modelling process, relatively satisfactory results are obtained in this paper. The predictive
291 performance of the output debris flow susceptibility maps, obtained from seventeen different models, is verified by
292 comparing with maps published by authority. By comparing the results, the following results are discussed:

293 Firstly, comparing R₁, R₂, R₃, R₄ and R₅, it can be concluded that the model based on field investigation and
294 expert experience is more effective than data-driven directly, when the information is insufficient. This is mainly
295 because when the basin area reaches a certain size, it is no longer controlled by one or several factors, but becomes
296 a complex system. It is not only the factors that affect the system, but also the system will react on each factor.
297 Geomorphic evolution is basically the result of the interaction of the endogenic and exogenic geological processes.
298 A geological period can be regarded as the beginning of an endogenic geological processes to the next one. In the
299 early stage of geological period, endogenic geological processes play a major role, and in the later relatively stable
300 period, exogenic geological processes will play a more and more important role. In this large cycle, the basin
301 continuously occurs a small cycle of accumulating and releasing energy, which leads to extremely complex system
302 changes. In addition, there is a contradiction between the scale of geological evolution and the scale of engineering
303 activities. So limited information can be obtained under these conditions that leads to the unreliability of data-driven
304 evaluation. Therefore, in the current period, field investigation and expert experience are fundamental.

305 Secondly, by comparing R₄ and R₅, R₆ and R₉, R₇ and R₁₀, R₈ and R₁₁, R₁₂ and R₁₅, R₁₃ and R₁₆, R₁₄ and R₁₇, it
306 can be concluded that the accuracy and resolution of the model can be improved by simplifying the factors, which
307 will eliminate the weak correlation and independence factors. In practical application, even if the susceptibility map
308 is obtained, the classification of the susceptibility degree is still a very difficult problem. Because everyone's
309 subjective definition of "susceptibility degree" is different. By simplifying the factors, the main factors can be selected,
310 which magnifies the differences between basins, so the boundaries between different susceptibility degrees are more
311 obvious.

312 Thirdly, by comparing R₆ and R₁₂, R₇ and R₁₃, R₈ and R₁₄, R₉ and R₁₅, R₁₀ and R₁₆, R₁₁ and R₁₇, it can be
313 concluded that the model in which factors are classified into two types is better than the method in which all factors
314 as a single thematic layer without classification. Because the factors categorized separately are more closely linked
315 and has consistent influence on the system in mechanism. We can also infer that the non-linear combination
316 characteristics between different types are stronger and scientific classification can improve the performance of the
317 model.

318 Fourthly, comparing R₁₂ and R₁₃, R₁₅ and R₁₆, it can be concluded that the frequency ratio method is better than
319 the cosine amplitude method in the study. Different from the study of (Kritikos and Davies, 2015), the watershed unit
320 rather than the grid unit is used, which indicates that the former has a wide range of application, while the latter has
321 a disadvantage of strict conditions.

322 Based on the results of the above four analyses, the most optimal model should have the features of being based
323 on expert experience, using selected factors, classifying factors before using them, and using frequency ratio method.
324 Then the model R₁₆ is selected according to the features, which is well in accordance with theoretical method
325 performance score, and gets fine mutual verification.

326 There is also much to discuss, the selection of factors is still a very complex dilemma. Although 19 factors
327 selected cannot fully evaluate the character of a basin, it is necessary to consider that they are easily and relatively

328 accurately obtainable for each basin. This will facilitate a wide range of applications. Besides, rainfall and total
329 amount of loose material source are also very important influencing factors. But according to the Beijing hydrological
330 manual, the rainfall change in the study area is not obvious, so it is not considered in model. And the total amount of
331 loose material source cannot be obtained for the watershed without on-site investigation, so calculations are
332 impossible. In fact, we indirectly consider the influence of natural loose material source by evaluating geological
333 conditions, but cannot consider the impact of human activities. As for the factors describing debris flow magnitude,
334 usually, several channels have the recorded data.

335 The scientific and systematic principle of model building is another challenge. To correctly classify the factors,
336 it is necessary to grasp the characteristics of the formation, movement and accumulation of debris flow. Therefore,
337 the classification should comprehensively consider the development background (geology, geomorphology, climate,
338 hydrology, soil, vegetation, human activities and other factors). The practical principle refers to that the study should
339 not only fully obtain scientific and accurate results, but also make the professional results understood by decision
340 makers. Although the susceptibility grade and susceptibility value of each watershed is obtained, the results are
341 relatively effective in this study area. In addition, with the development of technology and theory, we should replace
342 some traditional factors which are not easy to quantify with more precise quantitative factors to improve the efficiency
343 and accuracy of evaluation, such as surface roughness instead of drainage density.

344 For the results derived from Table 3, we would like to further discuss. It can be seen from the results that the
345 occurrence of debris flow is highly correlated with basin volume, basin area and main gully bending coefficient with
346 fuzzy membership above 0.7 in Beijing area. Rainfall in the study area is abundant to induce the debris flow. Loose
347 source and sinks the total volume of catchment become more important. The watershed area determines the total
348 volume of catchment. For the same rainfall, generally, the larger the area, the larger the catchment is. The bending
349 coefficient reflects the replenishment sources along the channel. The greater the coefficient, the slower the flow is.
350 Then loose source along the channel has more time to replenish. Basin volume characterizes the maximum amount
351 of loose material that can be supplied. These three features reflect the development characteristics of debris flow in
352 the study area. It also provides ideas for disaster prevention and mitigation.

353 **5 Conclusion**

354 In the present study, a new combination model for debris-flow susceptibility based on GIS was developed in
355 Pinggu. The objective and motivation of this study is to demonstrate a simple, extensible, and convenient analytical
356 model for the debris flow prediction. Three methods are selected in the model with their own advantages. GRA has
357 great advantages in the case of less samples, data-driven method is mainly used to reduce subjectivity and fuzzy
358 logic is fitted to solve nonlinear problems with fuzzy classification. The output debris flow susceptibility maps
359 obtained from the optimal models demonstrated satisfactory performance predicting approximately 50 % of the
360 debris flow gully with the relative higher susceptibility values corresponding to $AUC \geq 0.7$. Considering that the data
361 used for verification is only the recorded debris flow points rather than all debris flow records in the area, its
362 accuracy should be higher. The predictive performance of the susceptibility maps and the spatial correlation of
363 debris flow gully with H and VH susceptibility with recorded debris flow illustrate that the assessment at regional
364 scale using the proposed method is feasible. Compared with the previous results(Li et al., 2020b) based on grid

365 units in this area, the evaluation results are basically the same, but the model are more targeted for debris flow
366 disasters for decision makers. Besides, considering that the meaning of the used factors is clear and the data is easy
367 to obtain, these conditions mentioned enable the model to be widely applied.

368 Preliminary research indicates that: first of all, the evaluation results are obtained by combining the landslide
369 susceptibility analysis method with the debris flow. It reveals a systematic idea and disaster chain phenomenon.
370 Further more, we should pay more attention to the relative susceptibility value rather than absolute values in different
371 models, unless we need further study such as risk assessment. It is realized that the performance of the model is
372 determined by the effect of its classification. What's more, comprehensive consideration of endogenic and exogenic
373 geological processes in susceptibility assessment has better expected results. Last but not least, under the engineering
374 geological environment with acceptable difference, it has advantages of practical significance to regard the
375 administrative region as a research area for policy making, because different regions have different status constraints
376 in population quality and economy.

377 In short, an effort has been made to develop a cost- and time-efficient debris flow susceptibility assessment
378 model. The model has an acceptable degree of accuracy for regional-scale planning and contributes to susceptibility
379 and risk maps more accessible to individuals and local authorities. The GIS-based methods and modern data
380 availability especially through online databases are significantly beneficial to this aim. However, a challenge remains
381 in producing results with meaningful accuracy for the scale of planning, using available resources. Previous studies,
382 as well as the present work, highlight that the effectiveness of the final map depends on the quality of input data.
383 Comparison with a very high-resolution LIDAR-derived DEM indicated that the spatial accuracy of the DEM varies
384 between different landforms (lakes, river channels, riverbeds, floodplains etc.) and the areas of greatest errors are
385 predominantly confined to valley floors .However, with overall RMS error of 8.15 m, the DEM meets the
386 internationally accepted accuracy standards as set out by US Geological Survey (USGS 1997) and is of sufficient
387 quality for regional-scale studies such as the present one. Updating and improving existing debris flow catalogues
388 and inventories are crucial for the development of reliable susceptibility and risk assessment methods.

389 **Acknowledgements**

390 This research was financially supported by the Key Project of NSFC-Yunnan Joint Fund (Grant no. U1702241) and
391 the National Key Research and Development Plan (Grant No. 2018YFC1505301). The authors would like to thank Yuchao
392 Li, Zhihai Li, Jiejie Shen, Feifan Gu et al. for their contributions to the collection of field data, and the editor and anonymous
393 reviewers for their comments and suggestions which helped a lot in making this paper better.

394

395 **Reference**

- 396 Akbar, T. A. and Ha, S. R.: Landslide hazard zoning along Himalayan Kaghan Valley of Pakistan—by integration of GPS, GIS, and
397 remote sensing technology, *Landslides*, 8, 527-540, 10.1007/s10346-011-0260-1, 2011.
- 398 Benda, L. E.: Sediment routing by debris flow, 1987.
- 399 Benda, L. E. and Dunne, T.: Sediment routing by debris flow, in: *Erosion and sedimentation in the Pacific Rim*, edited by: Beschta, R.
400 L., Blinn, T., Grant, G. E., Swanson, F. J., and Ice, G. G., IAHS Publ, 213-223, doi:10.1111/j.1753-4887.1977.tb06503.x, 1987.
- 401 The distribution map of potential geological hazard points and susceptibility map in pinggu district:
402 http://ghzrzyw.beijing.gov.cn/zhengwuxinxi/zxzt/dzzhfztt/zzzhdcpj/202008/t20200807_1976436.html, last
403 Borrelli, L., Cofone, G., Coscarelli, R., and Gullà, G.: Shallow landslides triggered by consecutive rainfall events at Catanzaro strait
404 (Calabria–Southern Italy), *Journal of Maps*, 11, 730-744, 10.1080/17445647.2014.943814, 2014.
- 405 Bovis, M. and Dagg, B.: Debris flow triggering by impulsive loading - mechanical modeling and case-studies, *Canadian Geotechnical*
406 *Journal*, 29, 345-352, 10.1139/t92-040, 1992.
- 407 Cao, C., Xu, P., Chen, J., Zheng, L., and Niu, C.: Hazard assessment of debris-flow along the baicha river in heshigten banner, inner
408 mongolia, china, *Int J Environ Res Public Health*, 14, 1-19, 10.3390/ijerph14010030, 2016.
- 409 Chang, T. C. and Chien, Y. H.: The application of genetic algorithm in debris flows prediction, *Environmental Geology*, 53, 339-347,
410 10.1007/s00254-007-0649-2, 2007.
- 411 Chiou, I. J., Chen, C. H., Liu, W. L., Huang, S. M., and Chang, Y. M.: Methodology of disaster risk assessment for debris flows in a
412 river basin, *Stoch Env Res Risk A*, 29, 775-792, 10.1007/s00477-014-0932-1, 2015.
- 413 Chung, C.-J. F. and Fabbri, A. G.: Probabilistic prediction models for landslide hazard mapping, *Photogrammetric Engineering And*
414 *Remote Sensing*, 65, 1389-1399, 10.1016/S0924-2716(99)00030-1, 1999.
- 415 Chung, C. J. F., Fabbri, A., and Westen, C. J. v.: Multivariate regression analysis for landslide hazard zonation, *Geographical*
416 *Information Systems in Assessing Natural Hazards*, 5, 107-133, 1995.
- 417 Conoscenti, C., Ciaccio, M., Caraballo-Arias, N. A., Gómez-Gutiérrez, Á., Rotigliano, E., and Agnesi, V.: Assessment of susceptibility
418 to earth-flow landslide using logistic regression and multivariate adaptive regression splines: A case of the Belice River basin (western
419 Sicily, Italy), *Geomorphology*, 242, 49-64, 10.1016/j.geomorph.2014.09.020, 2015.
- 420 Crozier, M. J., Vaughan, E. E., and Tippett, J. M.: Relative instability of colluvium-filled bedrock depressions, *Earth Surface Processes*
421 *and Landforms*, 15, 329-339, 10.1002/esp.3290150404, 1990.
- 422 Dai, F. C. and Lee, C. F.: Landslide characteristics and slope instability modeling using GIS, Lantau Island, Hong Kong,
423 *Geomorphology*, 42, 213-228, 10.1016/S0169-555X(01)00087-3, 2002.
- 424 Dai, F. C., Lee, C. F., Li, H.-Z., and Xu, C.: Assessment of landslide susceptibility on the natural terrain of Lantau Island, Hong Kong,
425 *Environmental Geology*, 40, 381-391, 10.1007/s002540000163, 2001.
- 426 Deng, J. L.: Control problems of grey systems, *Systems and Control Letters*, 1, 288-294, 10.1016/S0167-6911(82)80025-X, 1982.
- 427 Deng, J. L.: *Grey prediction and decision*, Huazhong University of Science and Technology Press, Wuhan1988.
- 428 Di, B., Zhang, H., Liu, Y., Li, J., Chen, N., Stamatopoulos, C. A., Luo, Y., and Zhan, Y.: Assessing susceptibility of debris flow in
429 southwest china using gradient boosting machine, *Sci Rep*, 9, 12532, 10.1038/s41598-019-48986-5, 2019.
- 430 Di Napoli, M., Carotenuto, F., Cevasco, A., Confuorto, P., Di Martire, D., Firpo, M., Pepe, G., Raso, E., and Calcaterra, D.: Machine
431 learning ensemble modelling as a tool to improve landslide susceptibility mapping reliability, *Landslides*, 17, 1897-1914,
432 10.1007/s10346-020-01392-9, 2020.
- 433 Dietrich, W. E., Wilson, C. J., and Reneau, S. L.: Hollows, colluvium, and landslides in soil-mantled landscapes, in: *Hillslope*
434 *Processes*, edited by: Abrahams., A. D., Allen & Unwin, Boston, 1986.
- 435 Donati, L. and Turrini, M. C.: An objective method to rank the importance of the factors predisposing to landslides with the GIS
436 methodology: application to an area of the Apennines (Valnerina; Perugia, Italy), *Engineering Geology*, 63, 277-289, 10.1016/S0013-
437 7952(01)00087-4, 2002.
- 438 Dong, J.-J., Lee, C.-T., Tung, Y.-H., Liu, C.-N., Lin, K.-P., and Lee, J.-F.: The role of the sediment budget in understanding debris flow

439 susceptibility, *Earth Surface Processes and Landforms*, 34, 1612-1624, 10.1002/esp.1850, 2009.

440 Dramis, F. and Sorriso-Valvo, M.: Deep-seated gravitational slope deformations, related landslides and tectonics, *Engineering Geology*,

441 38, 231-243, 10.1016/0013-7952(94)90040-X, 1994.

442 Ercanoglu, M. and Gokceoglu, C.: Use of fuzzy relations to produce landslide susceptibility map of a landslide prone area (West Black

443 Sea Region, Turkey), *Engineering Geology*, 75, 229-250, 10.1016/j.enggeo.2004.06.001, 2004.

444 Ercanoglu, M. and Temiz, F. A.: Application of logistic regression and fuzzy operators to landslide susceptibility assessment in

445 Azdavay (Kastamonu, Turkey), *Environmental Earth Sciences*, 64, 949-964, 10.1007/s12665-011-0912-4, 2011.

446 Fairchild, L. H.: The importance of lahar initiation processes, *Reviews in Engineering Geology*, 7, 51-62, 10.1130/REG7-p51, 1987.

447 Fang, Z., Wang, Y., Peng, L., and Hong, H.: A comparative study of heterogeneous ensemble-learning techniques for landslide

448 susceptibility mapping, *International Journal of Geographical Information Science*, 35, 321-347, 10.1080/13658816.2020.1808897,

449 2020.

450 Frattini, P., Crosta, G., and Carrara, A.: Techniques for evaluating the performance of landslide susceptibility models, *Engineering*

451 *Geology*, 111, 62-72, 10.1016/j.enggeo.2009.12.004, 2010.

452 Gómez, H. and Kavzoglu, T.: Assessment of shallow landslide susceptibility using artificial neural networks in Jabonosa River Basin,

453 Venezuela, *Engineering Geology*, 78, 11-27, 10.1016/j.enggeo.2004.10.004, 2005.

454 Guzzetti, F., Carrara, A., Cardinali, M., and Reichenbach, P.: Landslide hazard evaluation: a review of current techniques and their

455 application in a multi-scale study, Central Italy, *Geomorphology*, 31, 181-216, 10.1016/s0169-555x(99)00078-1, 1999.

456 He, Y. and Beighley, R. E.: GIS-based regional landslide susceptibility mapping: a case study in southern California, *Earth Surface*

457 *Processes and Landforms*, 33, 380-393, 10.1002/esp.1562, 2008.

458 Hu, K., Wei, F., and Li, Y.: Real-time measurement and preliminary analysis of debris-flow impact force at Jiangjia Ravine, China,

459 *Earth Surface Processes and Landforms*, 36, 1268-1278, 10.1002/esp.2155, 2011.

460 Hungr, O., McDougall, S., and Bovis, M.: Entrainment of material by debris flows, in: *Debris-flow Hazards and Related Phenomena.*,

461 edited by: Jakob, M., and Hungr, O., Praxis.Springer Berlin Heidelberg, 135-158, 2005.

462 Iverson, R. M.: The physics of debris flows, *Reviews of Geophysics*, 35, 245-296., 10.1029/97RG00426, 1997.

463 Iverson, R. M., Reid, M. E., and LaHusen, R. G.: Debris-flow mobilization from landslides, *Annual Review of Earth and Planetary*

464 *Sciences*, 25, 85-138, 10.1146/annurev.earth.25.1.85, 1997.

465 Kanungo, D. P., Arora, M., Sarkar, S., and Gupta, R.: A fuzzy set based approach for integration of thematic maps for landslide

466 susceptibility zonation, *Georisk*, 3, 10.1080/17499510802541417, 2009.

467 Kanungo, D. P., Arora, M. K., Sarkar, S., and Gupta, R. P.: A comparative study of conventional, ANN black box, fuzzy and combined

468 neural and fuzzy weighting procedures for landslide susceptibility zonation in Darjeeling Himalayas, *Engineering Geology*, 85, 347-

469 366, 10.1016/j.enggeo.2006.03.004, 2006.

470 Kellogg, K. S.: Tectonic controls on a large landslide complex: Williams Fork Mountains near Dillon, Colorado, *Geomorphology*, 41,

471 355-368, 10.1016/S0169-555X(01)00067-8, 2001.

472 Khan, U., Tuteja, N. K., and Sharma, A.: Delineating hydrologic response units in large upland catchments and its evaluation using soil

473 moisture simulations, *Environmental Modelling & Software*, 46, 142-154, 10.1016/j.envsoft.2013.03.005, 2013.

474 Khan, U., Tuteja, N. K., Sharma, A., Lucas, S., Murphy, B., and Jenkins, B.: Applicability of Hydrologic Response Units in low

475 topographic relief catchments and evaluation using high resolution aerial photograph analysis, *Environmental Modelling & Software*,

476 81, 56-71, 10.1016/j.envsoft.2016.03.010, 2016.

477 Korup, O.: Geomorphic implications of fault zone weakening Slope instability along the Alpine Fault South Westland to Fiordland,

478 *New Zealand Journal of Geology and Geophysics*, 47, 257-267, 10.1080/00288306.2004.9515052, 2004.

479 Kritikos, T. and Davies, T.: Assessment of rainfall-generated shallow landslide/debris-flow susceptibility and runoff using a GIS-based

480 approach: application to western Southern Alps of New Zealand, *Landslides*, 12, 1051-1075, 10.1007/s10346-014-0533-6, 2015.

481 Kuo, Y., Yang, T., and Huang, G.-W.: The use of grey relational analysis in solving multiple attribute decision-making problems,

482 *Computers & Industrial Engineering*, 55, 80-93, 10.1016/j.cie.2007.12.002, 2008.

483 Lee, S.: Application and verification of fuzzy algebraic operators to landslide susceptibility mapping, *Environmental Geology*, 52, 615-
484 623, 10.1007/s00254-006-0491-y, 2006.

485 Lee, S. and Choi, J.: Landslide susceptibility mapping using GIS and the weight-of-evidence model, *International Journal of*
486 *Geographical Information Science*, 18, 789-814, 10.1080/13658810410001702003, 2004.

487 Lee, S. and Sambath, T.: Landslide susceptibility mapping in the Damrei Romel area, Cambodia using frequency ratio and logistic
488 regression models, *Environmental Geology*, 50, 847-855, 10.1007/s00254-006-0256-7, 2006.

489 Lee, S. and Talib, J. A.: Probabilistic landslide susceptibility and factor effect analysis, *Environmental Geology*, 47, 982-990,
490 10.1007/s00254-005-1228-z, 2005.

491 Lee, S., Ryu, J.-H., Min, K., and Won, J.-S.: Landslide susceptibility analysis using GIS and artificial neural network, *Earth Surface*
492 *Processes and Landforms*, 28, 1361-1376, 10.1002/esp.593, 2003.

493 Li, Y., Chen, J., Zhang, Y., Song, S., Han, X., and Ammar, M.: Debris flow susceptibility assessment and runout prediction: A case
494 study in shiyang gully, beijing, china, *International Journal of Environmental Research*, 14, 365-383, 10.1007/s41742-020-00263-4,
495 2020a.

496 Li, Y., Chen, J., Li, Z., Han, X., Zhai, S., Li, Y., and Zhang, Y.: A case study of debris flow risk assessment and hazard range prediction
497 based on a neural network algorithm and finite volume shallow water flow model, *Environmental Earth Sciences*, 80, 10.1007/s12665-
498 021-09580-z, 2021a.

499 Li, Y., Chen, J., Tan, C., Li, Y., Gu, F., Zhang, Y., and Mehmood, Q.: Application of the borderline-SMOTE method in susceptibility
500 assessments of debris flows in Pinggu District, Beijing, China, *Natural Hazards*, 105, 2499-2522, 10.1007/s11069-020-04409-7,
501 2020b.

502 Li, Z., Chen, J., Tan, C., Zhou, X., Li, Y., and Han, M.: Debris flow susceptibility assessment based on topo-hydrological factors at
503 different unit scales: a case study of Mentougou district, Beijing, *Environmental Earth Sciences*, 80, 10.1007/s12665-021-09665-9,
504 2021b.

505 Liang, W.-j., Zhuang, D.-f., Jiang, D., Pan, J.-j., and Ren, H.-y.: Assessment of debris flow hazards using a Bayesian Network,
506 *Geomorphology*, 171-172, 94-100, 10.1016/j.geomorph.2012.05.008, 2012.

507 Lin, C. L. and Lin, C. L.: The use of the orthogonal array with grey relational analysis to optimize the electrical discharge machining
508 process with multiple performance characteristics, *International Journal of Machine Tools and Manufacture*, 42, 237-244,
509 10.1016/S0890-6955(01)00107-9, 2002.

510 Liu, L. and Wang, S.: Fuzzy comprehensive evaluation on landslide and debris flow risk degree in Zaotong, Yunnan, *Mountain*
511 *Research*, 13, 261-266, 1995.

512 Liu, S., Dang, Y., and Fang, Z.: *Grey system theory and its applications*, Science Press, Beijing 2004.

513 Liu, Y., Guo, H. C., Zou, R., and Wang, L. J.: Neural network modeling for regional hazard assessment of debris flow in Lake
514 Qionghai Watershed, China, *Environmental Geology*, 49, 968-976, 10.1007/s00254-005-0135-7, 2005.

515 Lü, J., Wang, C., Liu, H., and Zhang, X.: Division of beijing geological environment system, *Urban geology*, 12, 19-25,
516 10.3969/j.issn.1007-1903.2017.03.004, 2017.

517 Luo, X. and Dimitrakopoulos, R.: Data-driven fuzzy analysis in quantitative mineral resource assessment, *Computers & Geosciences*,
518 29, 3-13, 10.1016/s0098-3004(02)00078-x, 2003.

519 Marjanović, M., Kovačević, M., Bajat, B., and Voženílek, V.: Landslide susceptibility assessment using SVM machine learning
520 algorithm, *Engineering Geology*, 123, 225-234, 10.1016/j.enggeo.2011.09.006, 2011.

521 Melo, R., Vieira, G., Caselli, A., and Ramos, M.: Susceptibility modelling of hummocky terrain distribution using the information
522 value method (Deception Island, Antarctic Peninsula), *Geomorphology*, 155-156, 88-95, 10.1016/j.geomorph.2011.12.027, 2012.

523 Meyer, N. K., Schwanghart, W., Korup, O., Romstad, B., and Etzel Müller, B.: Estimating the topographic predictability of debris
524 flows, *Geomorphology*, 207, 114-125, 10.1016/j.geomorph.2013.10.030, 2014.

525 Ohlmacher, G. C.: Plan curvature and landslide probability in regions dominated by earth flows and earth slides, *Engineering Geology*,
526 91, 117-134, 10.1016/j.enggeo.2007.01.005, 2007.

527 Pierson, T. C., Janda, R. J., Thouret, J.-C., and Borrero, C. A.: Perturbation and melting of snow and ice by the 13 November 1985
528 eruption of Nevado del Ruiz, Colombia, and consequent mobilization, flow and deposition of lahars, *Journal of Volcanology and*
529 *Geothermal Research*, 41, 17-66, 10.1016/0377-0273(90)90082-q, 1990.

530 Porwal, A., Carranza, E. J. M., and Hale, M.: A Hybrid Fuzzy Weights-of-Evidence Model for Mineral Potential Mapping, *Natural*
531 *Resources Research*, 15, 1-14, 10.1007/s11053-006-9012-7, 2006.

532 Pourghasemi, H. R., Yousefi, S., Kornejady, A., and Cerda, A.: Performance assessment of individual and ensemble data-mining
533 techniques for gully erosion modeling, *Sci Total Environ*, 609, 764-775, 10.1016/j.scitotenv.2017.07.198, 2017.

534 Pradhan, B.: Landslide susceptibility mapping of a catchment area using frequency ratio, fuzzy logic and multivariate logistic
535 regression approaches, *Journal of the Indian Society of Remote Sensing*, 38, 301-320, 10.1007/s12524-010-0020-z, 2010.

536 Pradhan, B.: Manifestation of an advanced fuzzy logic model coupled with Geo-information techniques to landslide susceptibility
537 mapping and their comparison with logistic regression modelling, *Environmental and Ecological Statistics*, 18, 471-493,
538 10.1007/s10651-010-0147-7, 2011a.

539 Pradhan, B.: Use of GIS-based fuzzy logic relations and its cross application to produce landslide susceptibility maps in three test
540 areas in Malaysia, *Environmental Earth Sciences*, 63, 329-349, 10.1007/s12665-010-0705-1, 2011b.

541 Regmi, N. R., Giardino, J. R., McDonald, E. V., and Vitek, J. D.: A comparison of logistic regression-based models of susceptibility to
542 landslides in western Colorado, USA, *Landslides*, 11, 247-262, 10.1007/s10346-012-0380-2, 2013.

543 Remondo, J., González, A., Terán, J. R. D. D., Cendrero, A., Fabbri, A., and Chung, C.-J. F.: Validation of landslide susceptibility
544 maps; examples and applications from a case study in northern Spain, *Natural Hazards*, 30, 437-449,
545 10.1023/B:NHAZ.0000007201.80743.fc, 2003.

546 Roeloffs, E.: Poroelastic techniques in the study of earthquake-related hydrologic phenomena, 38, 135-195, 10.1016/S0065-
547 2687(08)60270-8, 1996.

548 Ross, T. J.: *Fuzzy logic with engineering applications*, McGraw-Hill, New York 1995.

549 Selby, M. J.: *Hillslope materials and processes*, Oxford University Press, Oxford 1982.

550 Sun, X., Chen, J., Bao, Y., Han, X., Zhan, J., and Peng, W.: Landslide Susceptibility Mapping Using Logistic Regression Analysis
551 along the Jinsha River and Its Tributaries Close to Derong and Deqin County, Southwestern China, *ISPRS International Journal of*
552 *Geo-Information*, 7, 10.3390/ijgi7110438, 2018.

553 Takahashi, T.: *Debris flow mechanics, prediction and countermeasures*, second, Taylor & Francis/Balkema, The Netherlands 2014.

554 Tien Bui, D., Pradhan, B., Lofman, O., Revhaug, I., and Dick, O. B.: Landslide susceptibility assessment in the Hoa Binh province of
555 Vietnam: A comparison of the Levenberg–Marquardt and Bayesian regularized neural networks, *Geomorphology*, 171-172, 12-29,
556 10.1016/j.geomorph.2012.04.023, 2012.

557 Tsangaratos, P. and Ilia, I.: Landslide susceptibility mapping using a modified decision tree classifier in the Xanthi Prefecture, Greece,
558 *Landslides*, 13, 305-320, 10.1007/s10346-015-0565-6, 2015.

559 Tsukamoto, Y., Ohta, T., and Noguchi, H.: Hydrological and geomorphological studies of debris slides on forested hillslopes in Japan,
560 *Journal des Sciences Hydrologiques*, 27, 234, 1982.

561 Vallance, J. W. and Scott, K. M.: The Osceola mudflow from Mount Rainier: Sedimentology and hazard implications of a huge clay-
562 rich debris flow, *Geological Society of America Bulletin*, 109, 143-163, 10.1130/0016-7606(1997)109<0143:TOMFMR>2.3.CO;2,
563 1997.

564 Wang, J., Yu, Y., Yang, S., Lu, G.-h., and Ou, G.-q.: A modified certainty coefficient method (M-CF) for debris flow susceptibility
565 assessment: A case study for the Wenchuan earthquake meizoseismal areas, *Journal of Mountain Science*, 11, 1286-1297,
566 10.1007/s11629-013-2781-7, 2014.

567 Wei, Z., Shang, Y., Zhao, Y., Pan, P., and Jiang, Y.: Rainfall threshold for initiation of channelized debris flows in a small catchment
568 based on in-site measurement, *Engineering Geology*, 217, 23-34, 10.1016/j.enggeo.2016.12.003, 2017.

569 Westen, C. J. v., Rengers, N., and Soeters, R.: Use of geomorphological information in indirect landslide susceptibility assessment,
570 *Natural Hazards*, 30, 399-419, 10.1023/B:NHAZ.0000007097.42735.9e, 2003.

571 Wu, S., Chen, J., Zhou, W., Iqbal, J., and Yao, L.: A modified Logit model for assessment and validation of debris-flow susceptibility,
572 Bulletin of Engineering Geology and the Environment, 78, 4421-4438, 10.1007/s10064-018-1412-5, 2019.

573 Wu, Y., Li, W., Liu, P., Bai, H., Wang, Q., He, J., Liu, Y., and Sun, S.: Application of analytic hierarchy process model for landslide
574 susceptibility mapping in the Gangu County, Gansu Province, China, Environmental Earth Sciences, 75, 10.1007/s12665-015-5194-9,
575 2016.

576 Xie, H., Zhong, D., Wei, F., and Wang, S.: Classification of debris flow in the mountains of Beijing, Journal of mountain science, 22,
577 212-219, 10.16089/j.cnki.1008-2786.2004.02.013, 2004.

578 Zadeh, L. A.: Fuzzy sets, Information & Control, 8, 338-353, 10.1016/S0019-9958(65)90241-X, 1965.

579 Zhang, W., Li, H. Z., Chen, J. p., Zhang, C., Xu, L. m., and Sang, W. f.: Comprehensive hazard assessment and protection of debris
580 flows along Jinsha River close to the Wudongde dam site in China, Natural Hazards, 58, 459-477, 10.1007/s11069-010-9680-9, 2011.

581 Zhang, W., Chen, J.-p., Wang, Q., An, Y., Qian, X., Xiang, L., and He, L.: Susceptibility analysis of large-scale debris flows based on
582 combination weighting and extension methods, Natural Hazards, 66, 1073-1100, 10.1007/s11069-012-0539-0, 2013.

583 Zhang, Y., Chen, J., Tan, C., Bao, Y., Han, X., Yan, J., and Mehmood, Q.: A novel approach to simulating debris flow runout via a
584 three-dimensional CFD code: a case study of Xiaojia Gully, Bulletin of Engineering Geology and the Environment, 80, 5293-5313,
585 10.1007/s10064-021-02270-x, 2021.

586 Zhong, D., Xie, H., Wang, S., Wei, F., and Jin, H.: Debris flow in Beijing mountain, Commercial Press, Beijing2004.

587 Zou, Q., Cui, P., He, J., Lei, Y., and Li, S.: Regional risk assessment of debris flows in China—An HRU-based approach,
588 Geomorphology, 340, 84-102, 10.1016/j.geomorph.2019.04.027, 2019.

589